

## 飞秒激光焊接双层全钢化真空玻璃工艺研究

王红蕊<sup>1</sup>, 季羽飞<sup>1</sup>, 崔雪<sup>2\*\*\*</sup>, 刘庆京<sup>3</sup>, 刘博文<sup>1</sup>, 庞冬青<sup>1\*</sup>, 胡明列<sup>1\*\*</sup><sup>1</sup>天津大学精密仪器与光电子工程学院超快激光实验室, 天津 300072;<sup>2</sup>河北联纵工程管理咨询有限公司, 河北 沧州 062150;<sup>3</sup>北京莱泽光电技术有限公司, 北京 101300

**摘要** 通过自主设计的真空玻璃焊接治具,成功实现了基于飞秒激光器的钢化玻璃大面积焊接,并提出一种金属喷涂密封工艺来实现真空密封,进而研制出双层全钢化真空玻璃的生产设备。使用双层全钢化真空玻璃门窗替代现有的多层普通中空玻璃门窗,不仅可以减轻结构负荷、节约材料,还能延长门窗的使用寿命。该技术的普及应用将对实现我国的“双碳”目标产生积极影响。

**关键词** 飞秒激光; 玻璃焊接; 双层全钢化真空玻璃; 低碳环保

**中图分类号** O435 **文献标志码** A

**DOI:** 10.3788/CJL240760

## 1 引言

真空玻璃被广泛应用于建筑物、车船门窗和保温箱柜等领域。目前市场上的多层中空玻璃门窗受制作工艺的限制,多采用普通玻璃密封而成。双层全钢化真空玻璃相较于多层普通真空玻璃有着质量更轻、抗冲击性能更好、隔热隔音效果更好、使用寿命更长等优势,更符合节能减排、低碳环保的要求。现有的全钢化真空玻璃的制作方法使用高温焊接玻璃粉来实现密封,存在生产线较长、能耗较高、生产成本低以及玻璃钢化性质难以保证等问题,这些限制了全钢化真空玻璃的大规模生产。

在众多焊接技术中,飞秒激光焊接以其特殊的作用机制可以实现各种材料的焊接<sup>[1-4]</sup>。飞秒激光焊接不需要加入中间层材料,且超短脉冲特有的动力学过程<sup>[5]</sup>能够解决脆性玻璃材料易断裂的问题,焊接完成品的焊接强度接近于母材<sup>[6-7]</sup>。研究人员深入研究了飞秒激光焊接玻璃的过程及其动力学原理,揭示了飞秒激光焊接技术在玻璃焊接领域的显著优势和广阔应用前景。2005年,Tamaki等<sup>[8]</sup>使用波长为1558 nm、重复频率为500 kHz的飞秒脉冲,首次实现了非碱铝硅酸盐玻璃、非碱玻璃和硅片的焊接。Miyamoto等<sup>[9]</sup>于2014年使用波长为1045 nm、重复频率为100 kHz和1 MHz的飞秒激光实现了硼硅酸盐玻璃的焊接,并提出了热传导模型、等温区模拟和裂纹模型等理论,解释了焊接区域形貌的形成机理。

超快激光焊接玻璃通常要求两块玻璃的间隙小于

激光的四分之一波长<sup>[10]</sup>,因此在实验室中进行焊接研究实验时需要使用具有光学平整度的玻璃,其更容易实现表面贴合,达到上述间隙要求。2015年,Chen等<sup>[11]</sup>首次使用皮秒激光成功焊接了具有约3 μm间隙的硼硅酸盐玻璃和熔融硅。2020年,于森<sup>[12]</sup>使用75 W绿光飞秒激光器和255 mm长焦距振镜系统,实现了间隙约为3 μm的显示屏玻璃的非光学接触焊接,焊接强度可达20 MPa。2023年,陈观华等<sup>[13]</sup>使用飞秒激光脉冲成功焊接了表面平均粗糙度为5.2 nm、总厚度变化为10.4 μm的透明微晶玻璃,剪切强度达23.51 MPa。但是,与普通玻璃相比,钢化玻璃的表面平整度误差高达100 μm,因此一般的贴合方法不适用于钢化玻璃的焊接。

为了实现全钢化真空玻璃的工业化生产,本文设计了一种新型玻璃焊接治具,以实现钢化玻璃的大面积紧密贴合。利用波长为1030 nm、脉宽为378 fs、重复频率为1 MHz的飞秒激光器,成功焊接了尺寸为40 cm×40 cm的双层钢化玻璃。通过自主研发的真空玻璃金属喷涂技术,成功实现了大尺寸双层全钢化玻璃的真空密封。结果表明,该技术可以实现双层全钢化真空玻璃门窗的大批量工业化生产。

## 2 飞秒激光焊接装备

全钢化真空玻璃的飞秒激光焊接装备如图1所示。激光源为天津凯普林激光科技有限公司的BFL-1030-20L商用飞秒激光器,中心波长为1030 nm,脉宽为378 fs,重复频率为1 MHz,输出光斑直径为3 mm。自行研发的真空玻璃治具可高精度调平,被固定在二

收稿日期: 2024-04-11; 修回日期: 2024-05-20; 录用日期: 2024-06-13; 网络首发日期: 2024-06-24

通信作者: 国家自然科学基金(62227821)

通信作者: \*pangdongqing@tju.edu.cn; \*\*huminglie@tju.edu.cn; \*\*\*xuecui123@outlook.com

维移动平台上。加工物镜被固定在垂直于二维移动平台的一维移动平台上。输出的激光先后经过反射镜等

光学元件,最终通过数值孔径(NA)为0.4、工作距离为20 mm的聚焦物镜垂直入射到钢化玻璃内部。

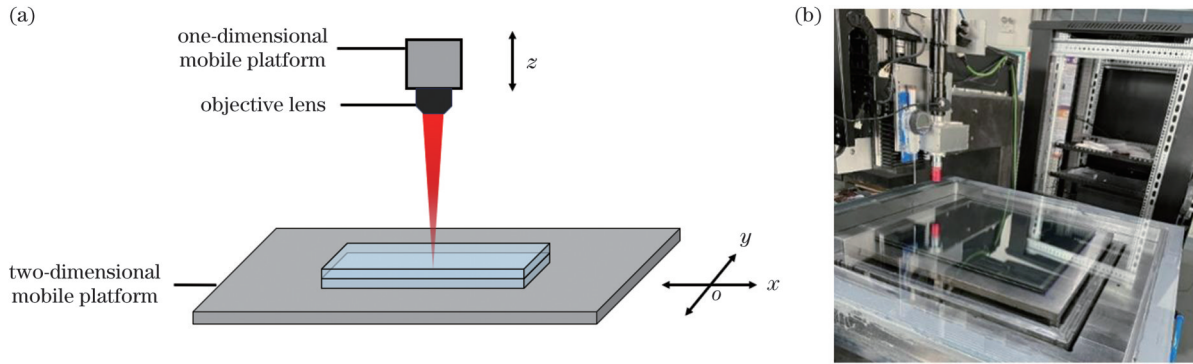


图1 实验装置及焊接装备。(a)实验装置示意图;(b)全钢化真空玻璃的自动化飞秒激光焊接装备实物图

Fig. 1 Experimental setup and welding equipment. (a) Schematic of experimental setup; (b) physical picture of automatic femtosecond laser welding equipment for fully tempered vacuum glass

玻璃的钢化过程导致玻璃表面平整度起伏约为100 μm,因此仅依靠螺栓紧固、活塞拉伸等机械运动方式进行贴合的工业冶具不能够满足钢化玻璃间大面积紧密贴合的要求。我们设计了一种通过抽真空挤压玻璃样品来实现大面积贴合的新型玻璃焊接冶具<sup>[14-15]</sup>,随后对该设计进行了优化,最终按照图2所示的设计方案<sup>[16-17]</sup>制作了焊接冶具,其中1(1')为夹具组件,10(10')为夹具,11(11')为气孔,12(12')为气缸,14(14')为上盖,16(16')为弹性件,20(20')为透明窗,22(22')为密封件,

90为待焊接工件。冶具的上表面为固定的玻璃窗口,便于飞秒激光通过并抵达加工区域。将一对可拆卸的夹具组件对接并围成封闭腔,用于放置待焊接工件。将夹具与上盖传动连接,带上盖向工件方向移动,以将工件夹持在透明窗之间。焊接前通过气缸上的气阀抽取腔内空气时,玻璃样品各位置都受到压力,从而实现钢化玻璃待加工区域的紧密贴合。利用腔内安装的水平度测量传感器和腔外的真空度测量传感器,动态控制腔内真空度,进而调整玻璃之间的贴合度。

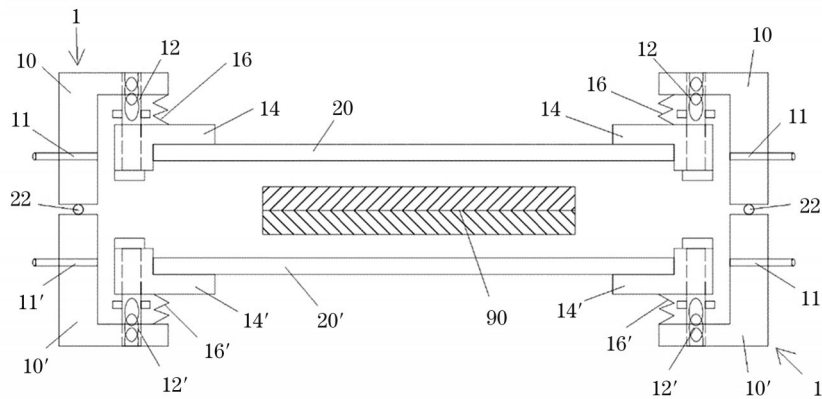


图2 新型激光焊接冶具<sup>[16-17]</sup>

Fig. 2 New laser welding fixture<sup>[16-17]</sup>

实验中使用的钢化玻璃尺寸为40.0 cm×40.0 cm×0.6 cm,中间层钢化玻璃边框的尺寸为40.0 cm×1.0 cm×0.1 cm,如图3所示。焊接完成后,顶层玻璃、底层玻璃会与中间层玻璃边框共同形成真空的密封空间<sup>[18-21]</sup>。为了避免在真空状态下顶层玻璃和底层玻璃发生变形,在待焊接的上下两块钢化玻璃间放置图3所示的玻璃支撑块阵列<sup>[22-23]</sup>。支撑块的直径为1 mm,高度与中间层玻璃保持一致。利用超快激光切割工艺可以批量快速制造支撑块,由于使用同样的钢化玻璃,支撑块在力学特性和光学特性上与上下层钢化玻璃一致,能够使焊接后的钢化真空玻璃具有良好的抗震和

透光特性。支撑块阵列的周期约为5.5 cm,该参数是基于双层全钢化真空玻璃的力学性能选取的<sup>[24]</sup>。冶具在焊接过程中通过从排气孔中抽取空气来实现真空状态。在该工艺中钢化玻璃在焊接前只需要进行简单的擦拭清洁,并不需要通过超声等手段达到光学清洁度,适用于工业生产的常规环境。

在焊接过程中首先焊接底层玻璃和中间层玻璃,再焊接中间层玻璃和顶层玻璃。如图4所示,焊接玻璃时应将激光束聚焦到玻璃交界面下方合适位置<sup>[5]</sup>(虚线),焦点区极高的激光功率密度导致产生多光子电离现象,继而发生雪崩电离,物质从电介质材料变为

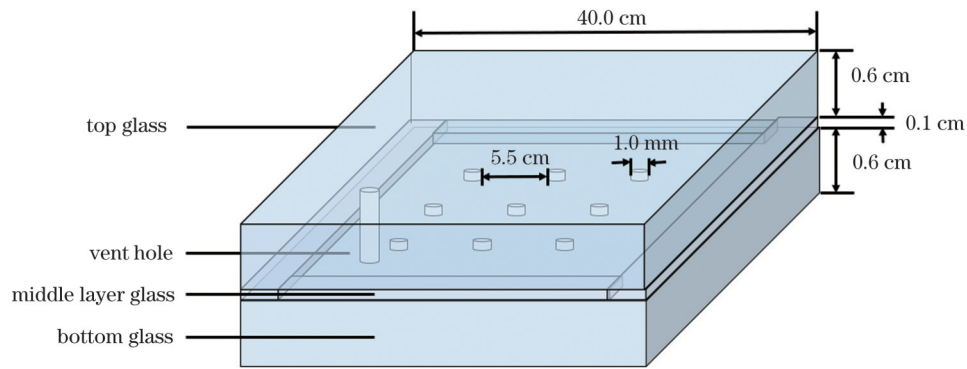


图 3 全钢化真空玻璃结构示意图

Fig. 3 Schematic of structure of fully tempered vacuum glass

等离子体<sup>[25]</sup>。等离子体对激光的吸收系数比玻璃高数个量级,因此等离子体区域自焦点位置迎向激光方向快速生长,直到激光功率密度下降到无法维持这种生长。等离子体冷却后形成中间的致密区,如图 4 中激光焦点上方的深色区域所示。同时,热扩散效应导致等离子体区域周边玻璃的温度快速升高至其熔点之上,形成水滴状的玻璃熔融区<sup>[26]</sup>,如图 4 中深色区域周围的浅色区域所示。当等离子体区域尺寸足够大时,会形成易被观测到的等离子体发光区,即图 4 中等离子体上部区域。实验证明,焦点的最佳位置应使得等离子体发光区域比较对称地分布在玻璃界面上下。因此在自动化飞秒激光焊接装备中可以引入侧边缘成像技术以快速寻找最优的焦点位置。这是一种易于观察和重复操作的寻找焦点最佳位置的方法,这种方法也适用于其他透明材料的焊接实验。与其他文献<sup>[11,27]</sup>所报道的一致,玻璃的焊接强度对焦点位置非常敏感,但是我们的实验证明,在不显著影响焊接强度的前提下,焦点的位置允许有 $\pm 10 \mu\text{m}$ 的偏离。由于

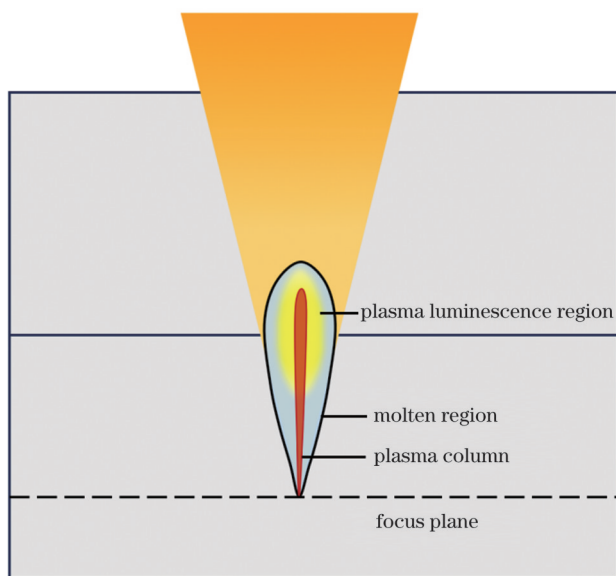


图 4 飞秒激光诱导等离子体发光区域的示意图

Fig. 4 Diagram of plasma luminescence region induced by femtosecond laser

钢化玻璃的平整度无法与光学玻璃比拟,较大的焦点位置允许度使得飞秒激光焊接钢化玻璃的工业生产成为可能。实验中在平均功率为 10 W 的条件下,加工速度可以高达 30 mm/s。

### 3 结果分析与讨论

玻璃贴合程度对焊接质量有决定性的影响。当厚度一定时,小尺寸样品的形变是由弹性力学决定的,而大尺寸样品的形变则是由非弹性力学决定的,因此样品尺寸越大,玻璃的贴合程度越好。我们利用两种不同的焊接工艺,即连续扫描式焊接和断续扫描式焊接,对较大尺寸的钢化玻璃样品进行了焊接。连续扫描式焊接的焊接区域形貌如图 5(a)、(b)所示,焊接区域的焊线是完全连续的。我们的实验显示,如果两块玻璃不存在间隙,就不会在光学显微镜下出现可被观测到的烧蚀和裂纹,如图 5(a)所示。这是因为此时两块玻璃可以看作一个整体,迎向激光方向的等离子体的生长是连续的。图 5(b)是焊接失败时直接观测玻璃界面的结果,玻璃的表面出现大量的烧蚀和微细的裂纹,大部分烧蚀区域的长度达到焊线宽度的两倍。在显微镜下,黑色烧蚀区总是聚集性出现的,我们认为这是由于该处在厘米级长度范围内出现贴合间隙。当两块玻璃界面存在间隙时,等离子体会向四周扩散,等离子体密度迅速下降,从而较易导致表面烧蚀和裂纹的产生。此时等离子体就无法迎向激光方向连续生长,导致图 4 所示的焊接动力学的中断。综上所述,间隙是影响飞秒激光焊接玻璃效果最为关键的要素。

通过精确控制激光的通断可以进行断续扫描式焊接,图 5(c)和图 5(d)是焊线的占空比为 7:3 时的结果。图 5(c)是成功焊接时的显微照片,焊接区和玻璃区之间的明显边界可能是折射率突变造成的。图 5(d)情况比较复杂,焊接区和玻璃区的边界线较图 5(c)情况更加明显,且存在一些黑色的微小烧蚀和裂纹区域,但其长度几乎没有超过焊线宽度。我们认为这样的区域焊接强度不如图 5(c)的结果,但也成功实现了焊接。

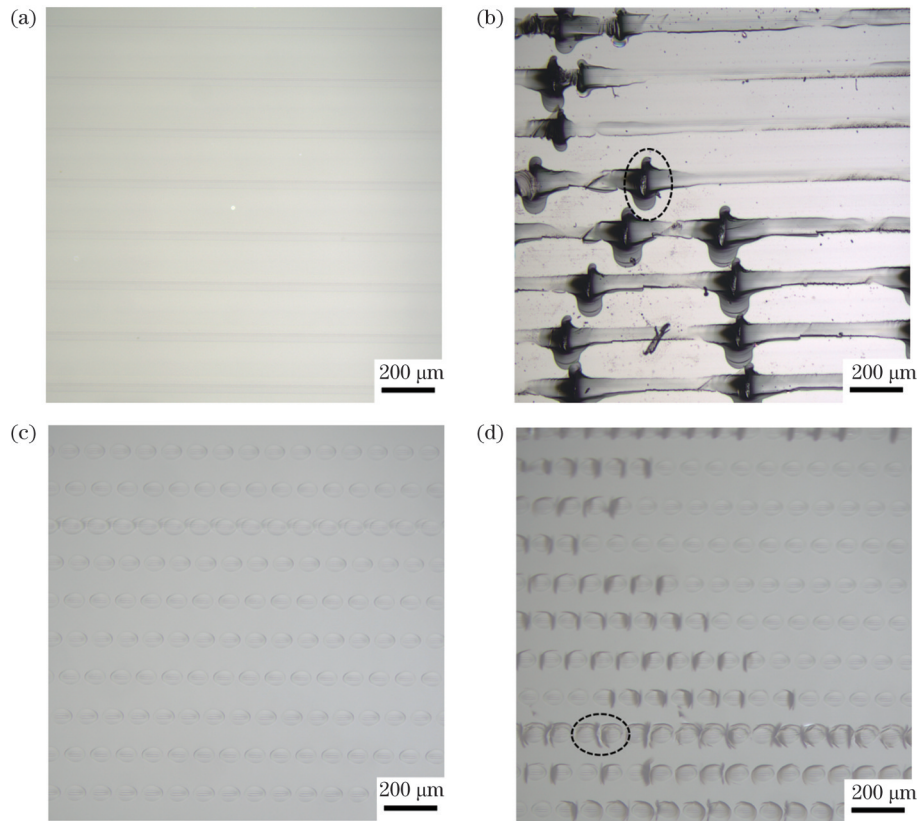


图 5 全钢化真空玻璃焊接样品的焊接区域在光学显微镜下的照片。(a)连续扫描式焊接工艺下不存在烧蚀和裂纹的焊接区域；(b)连续扫描式焊接工艺下焊接失败的玻璃表面；(c)断续扫描式焊接工艺下不存在烧蚀和裂纹的焊接区域；(d)断续扫描式焊接工艺下存在轻微烧蚀和微细裂纹的焊接区域

Fig.5 Morphologies of welding areas of fully tempered vacuum glass welding samples observed by optical microscope. (a) Welding area without ablation and cracks under continuous scanning welding process; (b) surface of glass that fails to be welded under continuous scanning welding process; (c) welding area without ablation and cracks under intermittent scanning welding process; (d) welding area with slight ablation and cracks under intermittent scanning welding process

下文的推拉实验(图6)证明,即使存在这样微小的烧蚀和裂纹区,断裂面并不在图5(d)所示的区域内。因此,通过光学显微镜照片可以初步判断焊接的成功与否,这使得在实际加工中可以原位监测加工效果。上述实验结果也证明,断续扫描式焊接相较连续扫描式焊接更容易实现大面积的焊接。我们的冶具能确保钢化玻璃的大面积紧密贴合,但并不能实现百分之百的完美贴合,所以在工业生产中总会存在微观局域的间隙。实验证明,只要将烧蚀和裂纹区的占比控制在一定比例之下,就可以实现焊接强度的长期稳定性。焊接完成后的样品在静置一年后没有发生分离或开裂,在经过长程跨省运输和随意搬动后,也未发生任何破损。

为了测试样品的焊接强度,在断续扫描工艺焊接的玻璃样品上使用北京莱泽光电技术有限公司的MLPS-II贝塞尔飞秒激光随机切割出三块尺寸约为1.0 cm×1.5 cm的小型样品,使用图6(a)所示的荷兰XYZTEC公司的Conder 150多功能推拉力测试仪进行了剪切强度的测试。测试中样品被固定在实验台上,使用推头推进焊接区上层的玻璃,直至两块玻璃间发生断裂。剪切强度<sup>[28]</sup>( $\sigma$ )的计算公式为

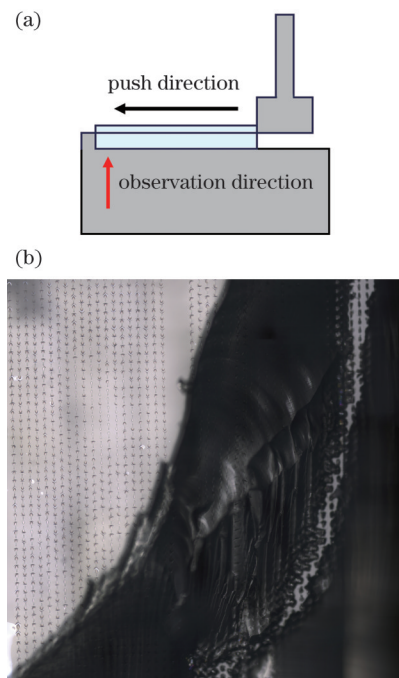


图 6 推拉实验。(a)推拉测试原理图;(b)测试样品的断裂情况  
Fig.6 Push-pull experiment. (a) Schematic diagram of push-pull test; (b) fracture of tested sample

$$\sigma = \frac{F}{S_{\text{weld}}}, \quad (1)$$

式中:  $F$  表示推力;  $S_{\text{weld}}$  表示焊接区域总面积。通常情况下, 钢化玻璃母材的剪切强度与普通玻璃差别不大。通过计算得到三个样品的剪切强度均约为 10 MPa。使用光学显微镜沿图 6(a) 所示的观测方向进行观测, 得到了图 6(b) 所示的断裂面对应的部分焊接面(即两玻璃的交界面)的形貌。可以看到, 即使焊接区域存在较多的微观烧蚀和裂纹区域, 样品的焊接强度仍较高, 断裂发生在焊接区域周围, 而不是在两块玻璃的原始交界面处。这是因为如文献[6-7]证明的, 飞秒激光的玻璃焊接强度可以接近母材, 所以焊接强度主要受控于烧蚀区域和裂纹的密度。对于大面积的玻璃焊接来说, 焊接强度主要受控于贴合度的完全性, 控制烧蚀和裂纹区域占总焊接区域的比例就能确保工业生产所需的焊接强度。

图 7 为焊接后的全钢化真空玻璃实物图。使用美国 PerkinElmer 公司的 LAMBDA 750 紫外可见近红外分光光度计, 分别测试了焊接样品和玻璃原样在 300~800 nm 波段的透过率。用于测试的玻璃原样选择了 5 mm 厚的钢化玻璃。每个样品都随机选取了多个不同区域进行测试。测试结果表明, 焊接后样品和玻璃原样的透明范围为 375~800 nm。透过率的测量结果受玻璃散射的影响, 由于我们并不能保证每个检测区域的散射是完全相同的, 因此我们将不同区域的透过率进行了平均处理。下面的测试结果没有扣除表面反射。在 375 nm 处, 玻璃原样的透过率为 82.6%, 焊接样品的透过率为 78.7%, 较玻璃原样下降了 3.9%。在 800 nm 处两样品的透过率均为最低值, 玻璃样品的透过率为 70.2%, 焊接样品的透过率为 68.6%, 较玻璃原样仅下降 1.6%。玻璃样品在 610 nm 处的透过率达到最大值, 为 87.2%, 焊接样品在 540 nm 处的透过率达到最大值, 为 85.7%。焊接样品在整个

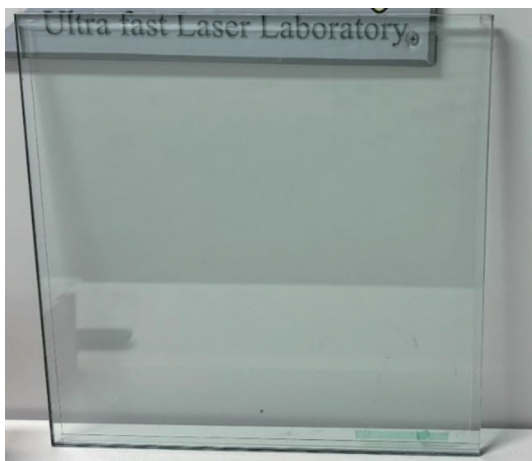


图 7 焊接后的全钢化真空玻璃实物图(40 cm×40 cm)

Fig. 7 Physical image of fully tempered vacuum glass after welding (40 cm×40 cm)

透明波段较原样透过率的下降小于 4.4%。由此可见, 焊接完成后的区域仍然表现出良好的光学透明度。从透过率曲线还能够估算出该钢化玻璃的光学带隙约为 3.5 eV。

由于钢化玻璃的平整度较低, 完全通过激光焊接来实现真空密封对焊接工艺的要求过高, 因此设计了一种低熔点金属涂覆工艺来辅助实现真空密封<sup>[29-32]</sup>。将液态金属铟均匀涂覆在焊接完成后的钢化玻璃侧面。金属铟完全覆盖焊接区域, 在与钢化玻璃侧面充分浸润结合后形成金属薄膜。利用自主设计的超声压焊装置在钢化玻璃侧面进行摩擦, 使得金属铟薄膜与钢化玻璃紧密贴合, 从而既更好满足了真空度要求, 又实现了真空度的长期稳定性, 最终的密封效果如图 8 所示。这种低成本且简易的喷涂密封工艺, 降低了飞秒激光焊接全钢化真空玻璃自动化生产线的技术要求, 使得本文设计的全套技术方案适用于工业化大规模生产。

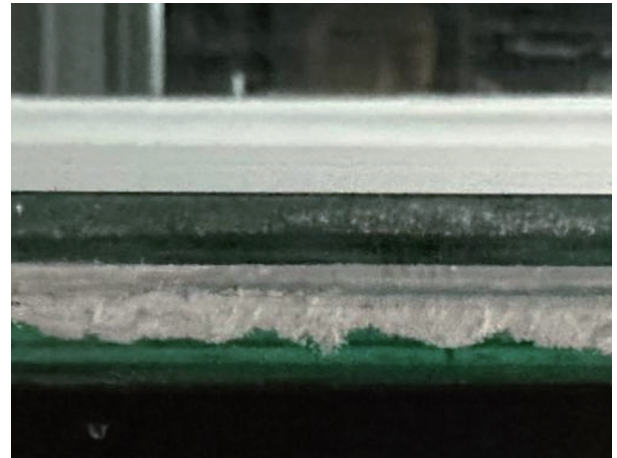


图 8 全钢化真空玻璃喷涂铟封后的侧面照片

Fig. 8 Photo of side of fully tempered vacuum glass sprayed and sealed with indium

## 4 结 论

利用自主研发的真空玻璃焊接治具, 成功解决了两块钢化玻璃间的大面积紧密贴合问题, 进而研制成功了飞秒激光焊接全钢化真空玻璃自动化生产设备, 并实现了尺寸为 40 cm×40 cm 的钢化玻璃的大面积焊接。自主设计了一种低熔点金属薄膜涂覆工艺, 实现了全钢化真空玻璃的长期真空密封。本文报道的飞秒激光焊接钢化真空玻璃的技术方案, 具有设备成本低、工艺简单的优势, 适用于工业化大规模生产。该技术方案符合国家节能减排、低碳经济的战略目标, 是未来制造低能耗的绿色建筑物、车船门窗及保温箱柜的最优选择之一。目前正在中试尺寸为 1.5 m×3.0 m 的飞秒激光焊接设备, 以实现更大面积的全钢化真空玻璃的制作, 推动工业化生产。

## 参 考 文 献

- [1] Choi H, Nguyen P T, Bin In J. *Laser transmission welding and surface modification of graphene film for flexible supercapacitor applications*[J]. *Applied Surface Science*, 2019, 483: 481-488.
- [2] Richter S, Döring S, Tünnermann A, et al. *Bonding of glass with femtosecond laser pulses at high repetition rates*[J]. *Applied Physics A*, 2011, 103(2): 257-261.
- [3] Horn A, Mingareev I, Werth A, et al. *Investigations on ultrafast welding of glass - glass and glass - silicon*[J]. *Applied Physics A*, 2008, 93(1): 171-175.
- [4] Ozeki Y, Inoue T, Tamaki T, et al. *Direct welding between copper and glass substrates with femtosecond laser pulses*[J]. *Applied Physics Express*, 2008, 1(8): 082601.
- [5] Kaiser E. *Laser welding of glass replaces glueing procedure*[J]. *Laser Technik Journal*, 2016, 13(3): 22-25.
- [6] Miyamoto I, Cvecek K, Okamoto Y, et al. *Characteristics of laser absorption and welding in FOTURAN glass by ultrashort laser pulses*[J]. *Optics Express*, 2011, 19(23): 22961-22973.
- [7] 丁腾, 王雪辉, 王关德, 等. *高重频飞秒激光焊接石英玻璃*[J]. *中国激光*, 2018, 45(7): 0701007.  
Ding T, Wang X H, Wang G D, et al. *Welding of fused silica by using high repetition frequency femtosecond laser*[J]. *Chinese Journal of Lasers*, 2018, 45(7): 0701007.
- [8] Tamaki T, Watanabe W, Nishii J, et al. *Welding of transparent materials using femtosecond laser pulses*[J]. *Japanese Journal of Applied Physics*, 2005, 44(5L): L687-L689.
- [9] Miyamoto I, Cvecek K, Okamoto Y, et al. *Internal modification of glass by ultrashort laser pulse and its application to microwelding*[J]. *Applied Physics A*, 2014, 114(1): 187-208.
- [10] Cvecek K, Miyamoto I, Strauss J, et al. *Sample preparation method for glass welding by ultrashort laser pulses yields higher seam strength*[J]. *Applied Optics*, 2011, 50(13): 1941-1944.
- [11] Chen J Y, Carter R M, Thomson R R, et al. *Avoiding the requirement for pre-existing optical contact during picosecond laser glass-to-glass welding*[J]. *Optics Express*, 2015, 23(14): 18645-18657.
- [12] 于淼. *长焦距绿光飞秒激光玻璃微焊接工艺研究*[D]. 北京: 北京工业大学, 2020.  
Yu M. *Study on micro-welding technology of long focal green femtosecond laser glass*[D]. Beijing: Beijing University of Technology, 2020.
- [13] 陈观华, 肖蒲庐, 张翔, 等. *飞秒激光脉冲焊接透明微晶玻璃的实验研究*[J]. *中国激光*, 2023, 50(16): 1602104.  
Chen G H, Xiao P L, Zhang X, et al. *Experimental study on transparent glass-ceramic welding with femtosecond laser pulses*[J]. *Chinese Journal of Lasers*, 2023, 50(16): 1602104.
- [14] 崔晓晓. *一种激光焊接治具*: CN113523619A[P]. 2021-10-22.  
Cui X X. *A laser welding fixture*: CN113523619A[P]. 2021-10-22.
- [15] 崔晓晓. *一种激光焊接治具*: CN218169113U[P]. 2022-12-30.  
Cui X X. *A laser welding fixture*: CN218169113U [P]. 2022-12-30.
- [16] 崔晓晓. *一种激光焊接治具*: CN113695740A[P]. 2021-11-26.  
Cui X X. *A laser welding fixture*: CN113695740A[P]. 2021-11-26.
- [17] 崔晓晓. *一种激光焊接治具*: CN215919414U[P]. 2022-03-01.  
Cui X X. *A laser welding fixture*: CN215919414U[P]. 2022-03-01.
- [18] 崔玉柱, 崔岳, 闫锋, 等. *真空密封的钢化真空玻璃及钢化玻璃真空密封方法*: CN115304293A[P]. 2022-11-08.  
Cui Y Z, Cui Y, Yan F, et al. *Vacuum sealed tempered vacuum glass and vacuum sealing method for tempered glass*: CN115304293A[P]. 2022-11-08.
- [19] 崔玉柱, 崔岳, 闫锋, 等. *真空密封的钢化真空玻璃*: CN218174836U[P]. 2022-12-30.  
Cui Y Z, Cui Y, Yan F, et al. *Vacuum sealed tempered vacuum glass*: CN218174836U[P]. 2022-12-30.
- [20] 崔玉柱, 崔晓晓, 闫锋, 等. *一种真空密封钢化玻璃及其制作方法*: CN116444180A[P]. 2023-07-18.  
Cui Y Z, Cui X X, Yan F, et al. *A vacuum sealed tempered glass and its production method*: CN116444180A[P]. 2023-07-18.
- [21] 崔玉柱, 崔晓晓, 闫锋, 等. *一种真空密封钢化玻璃*: CN220056666U[P]. 2023-11-21.  
Cui Y Z, Cui X X, Yan F, et al. *A type of vacuum sealed tempered glass*: CN220056666U[P]. 2023-11-21.
- [22] 崔玉柱, 崔鹏程, 李鼎顺, 等. *钢化真空玻璃内部支撑块布放装置及方法*: CN115142768A[P]. 2022-10-04.  
Cui Y Z, Cui P C, Li D S, et al. *Layout device and method for internal support blocks of tempered vacuum glass*: CN115142768A [P]. 2022-10-04.
- [23] 崔玉柱, 崔鹏程, 李鼎顺, 等. *钢化真空玻璃内部支撑块布放装置*: CN218581472U[P]. 2023-03-07.  
Cui Y Z, Cui P C, Li D S, et al. *Layout device for internal support blocks of tempered vacuum glass*: CN218581472U[P]. 2023-03-07.
- [24] 李彦兵, 岳高伟. *钢化真空玻璃支撑点的排布方式*[J]. *材料科学与工程学报*, 2016, 34(6): 955-959, 966.  
Li Y B, Yue G W. *Support point arrangement of tempered vacuum glass*[J]. *Journal of Materials Science and Engineering*, 2016, 34(6): 955-959, 966.
- [25] Stuart B C, Feit M D, Herman S, et al. *Nanosecond-to-femtosecond laser-induced breakdown in dielectrics*[J]. *Physical Review B*, 1996, 53(4): 1749-1761.
- [26] Miyamoto I, Cvecek K, Schmidt M. *Crack-free conditions in welding of glass by ultrashort laser pulse*[J]. *Optics Express*, 2013, 21(12): 14291-14302.
- [27] Richter S, Zimmermann F, Eberhardt R, et al. *Toward laser welding of glasses without optical contacting*[J]. *Applied Physics A*, 2015, 121(1): 1-9.
- [28] Alexeev I, Cvecek K, Schmidt C, et al. *Characterization of shear strength and bonding energy of laser produced welding seams in glass*[J]. *Journal of Laser Micro/Nanoengineering*, 2012, 7(3): 279-283.
- [29] 崔玉柱, 崔鹏程, 李鼎顺, 等. *低熔点金属薄膜涂覆设备及方法*: CN115125534A[P]. 2022-09-30.  
Cui Y Z, Cui P C, Li D S, et al. *Low melting point metal film coating equipment and methods*: CN115125534A[P]. 2022-09-30.
- [30] 崔玉柱, 崔鹏程, 李鼎顺, 等. *低熔点金属薄膜涂覆设备*: CN218756039U[P]. 2023-03-28.  
Cui Y Z, Cui P C, Li D S, et al. *Low melting point metal film coating equipment*: CN218756039U[P]. 2023-03-28.
- [31] 崔玉柱, 崔晓晓, 闫锋, 等. *一种带助焊涂层的焊接组件*: CN220636613U[P]. 2024-03-22.  
Cui Y Z, Cui X X, Yan F, et al. *A welding component with welding flux coating*: CN220636613U[P]. 2024-03-22.
- [32] 崔玉柱, 崔晓晓, 闫锋, 等. *一种带助焊涂层的焊接组件及焊接组件制备方法*: CN117961275A[P]. 2024-05-03.  
Cui Y Z, Cui X X, Yan F, et al. *A welding component with a welding flux coating and a preparation method for welding components*: CN117961275A[P]. 2024-05-03.

# Femtosecond Laser Welding of Double-Layer Fully Tempered Vacuum Glass

Wang hongrui<sup>1</sup>, Ji Yufei<sup>1</sup>, Cui Xue<sup>2\*\*\*</sup>, Liu Qingjing<sup>3</sup>, Liu Bowen<sup>1</sup>, Pang Dongqing<sup>1\*</sup>, Hu Minglie<sup>1\*\*</sup>

<sup>1</sup>Ultrafast Laser Laboratory, School of Precision Instrument and Optoelectronics Engineering, Tianjin

University, Tianjin 300072, China;

<sup>2</sup>Hebei Lianzong Engineering Management Consulting Co., Ltd., Cangzhou 062150, Hebei, China;

<sup>3</sup>Beijing Laize Photonics Co., Ltd., Beijing 101300, China

## Abstract

**Objective** Multilayer hollow glass is widely used in the doors and windows of buildings, vehicles, ships, and incubators. Fully tempered vacuum glass possesses all the characteristics of vacuum glass, and has better thermal insulation performance, higher impact strength, and better resistance to rapid cooling and healing. Currently, owing to the limitations of the tempering process and edge-sealing technology, tempered glass cannot be used for the large-scale industrial production of vacuum glass doors and windows. Direct femtosecond (fs) laser welding of glass can achieve high welding strength without generating cracks. This method typically requires a gap not exceeding a few micrometers between two pieces of glass. However, the extremely low surface flatness of tempered glass renders such close contact impossible if holding methods reported in references are used. Herein, we report a self-designed glass-welding vacuum fixture to achieve large-area close contact between two pieces of stacked tempered glass. Using this device, we successfully achieve the large-area welding of tempered glass by employing fs laser pulses. A metal spray-sealing process is developed to obtain vacuum sealing. This self-developed double-layer-tempered-vacuum-glass production equipment based on fs laser welding is both simple and affordable, which is consistent with the goals of energy saving and low-carbon environmental protection.

**Methods** Figure 1 shows automatic fs laser welding equipment used for fully tempered vacuum glass welding. A self-designed special welding fixture (Fig. 2) is fixed to a two-dimensional mobile platform. The fixture makes tempered glass contact tightly with each other by properly squeezing the glass plates through adjusting the vacuum pumping. The tempered glass measures 40.0 cm × 40.0 cm × 0.6 cm and the tempered glass used for the middle frame layer measures 40.0 cm × 1.0 cm × 0.1 cm (Fig. 3). Additionally, to avoid the deformation of the top and bottom glass layers in vacuum, an array of glass pillars (diameter of 1 mm) is placed between two tempered glass plates. Before welding, the tempered glass only requires simple wiping and cleaning. The welding process is implemented twice. The bottom glass and middle-frame-layer glass are welded first, followed by the middle glass and top glass. Experimental results show that the optimal focal position should result in a symmetric distribution of the plasma luminescence region across the interface between the two pieces of glass (Fig. 4). Successful large-area welding is achieved at a power of 10 W and a welding speed of 30 mm/s.

**Results and Discussions** Figure 5 shows the importance of controlling the gap between two pieces of glass. No ablation regions or cracks are observed in the welding region when no gaps are present between the two pieces of glass. Welding fails when a gap is present because ablation occurs when the plasma plume can expand freely in the gap space. Cracks typically emerge in this case. It is essential that the plasma region must continuously grow only toward the laser. Furthermore, the experimental results show that the interrupted-scanning welding process can achieve successful large-area welding more easily compared with continuous-scanning welding. In the interrupted-scanning case, we randomly cut three small samples from one welded sample and measured their shear strengths. The average shear strength is approximately 10 MPa. Results of the push-pull test show that even in the presence of a few micro-sized ablation zones and micro-sized crack zones, the fracture surface is not at the original interface between the two pieces of glass (Fig. 6). We cannot guarantee 100% perfect contact of the tempered glass; however, our results of long-term stability testing show that a small number of micro-sized ablation regions and cracks are allowable. The optical band gap of the tempered glass is approximately 3.5 eV. The decrease in transmittance of the welded sample over the entire transparent range (375–800 nm) is less than 4.4% compared with that of the tempered glass. After welding, the samples maintain their good optical transparency (Fig. 7). The fully tempered vacuum glass is sealed with indium (Fig. 8), which improves the vacuum level and alleviates the technical requirements of fs laser welding automation production line.

**Conclusions** Herein, we report a self-designed vacuum glass-welding fixture to solve the problem of large-area close contact between two pieces of tempered glass. We successfully develop production equipment for the fs laser welding of fully tempered vacuum glass. Using this equipment, we fabricate a 40 cm × 40 cm sample. Low-melting-point metal coating equipment is designed and tested. The technical solution proposed in this study for welding tempered vacuum glass using a fs laser offers the advantages of reducing the equipment cost and simplifying the production process, thus rendering it suitable for large-scale industrial production. This technical solution is consistent with the global goals of energy conservation, emission reduction, and low-carbon economy. In fact, it is one of the best options for manufacturing low-energy green doors and windows for buildings, vehicles, ships, and incubators. Currently, automated fs laser welding equipment with dimensions of 1.5 m × 3.0 m is being pilot tested to prepare for its industrial production.

**Key words** femtosecond laser; glass welding; double-layer fully tempered vacuum glass; low-carbon environmental protection